

# c-Jun N-terminal Kinase Regulates Soluble A $\beta$ Oligomers and Cognitive Impairment in AD Mouse Model<sup>\*[5]</sup>

Received for publication, August 25, 2011, and in revised form, October 17, 2011. Published, JBC Papers in Press, October 27, 2011, DOI 10.1074/jbc.M111.297515

Alessandra Sclip<sup>†1</sup>, Xanthi Antoniou<sup>†1</sup>, Alessio Colombo<sup>‡</sup>, Giovanni G. Camici<sup>§</sup>, Laura Pozzi<sup>‡</sup>, Daniele Cardinetti<sup>‡</sup>, Marco Feligioni<sup>‡</sup>, Pietro Veglianesi<sup>‡</sup>, Ferdinand H. Bahlmann<sup>¶</sup>, Luigi Cervo<sup>‡</sup>, Claudia Balducci<sup>‡</sup>, Cinzia Costa<sup>||</sup>, Alessandro Tozzi<sup>||</sup>, Paolo Calabresi<sup>||\*\*</sup>, Gianluigi Forloni<sup>‡</sup>, and Tiziana Borsello<sup>†2</sup>

From the <sup>†</sup>Neuronal Death and Neuroprotection Laboratory, Department of Neuroscience, Mario Negri Institute for Pharmacological Research, Milano 20156, Italy, the <sup>§</sup>Cardiovascular Research Laboratory, Institute of Physiology, University of Zurich, Zurich 8057, Switzerland, the <sup>¶</sup>Department of Internal Medicine IV, Saarland University Medical Centre, 66421 Homburg/Saar, Germany, the <sup>||</sup>Clinica Neurologica Division, Università di Perugia, Ospedale S. Maria della Misericordia, Perugia 06156, Italy, and <sup>\*\*</sup>Fondazione Santa Lucia, Istituto di Ricovero e Cura a Carattere Scientifico, Rome 00143, Italy

**Background:** Neuropathological mechanisms in Alzheimer disease (AD) are partially unknown.

**Results:** Chronic JNK inhibition with a cell-permeable peptide (CPP) rescues memory deficits, LTP impairment, and reduces A $\beta$  oligomers in a mouse model that mimics AD.

**Conclusion:** JNK is crucial in AD neurodegenerative mechanisms.

**Significance:** CPPs offer an important tool to interfere with neurodegeneration. JNK is a promising target against AD.

Alzheimer disease (AD) is characterized by cognitive impairment that starts with memory loss to end in dementia. Loss of synapses and synaptic dysfunction are closely associated with cognitive impairment in AD patients. Biochemical and pathological evidence suggests that soluble A $\beta$  oligomers correlate with cognitive impairment. Here, we used the TgCRND8 AD mouse model to investigate the role of JNK in long term memory deficits. TgCRND8 mice were chronically treated with the cell-penetrating c-Jun N-terminal kinase inhibitor peptide (D-JNKI1). D-JNKI1, preventing JNK action, completely rescued memory impairments (behavioral studies) as well as the long term potentiation deficits of TgCRND8 mice. Moreover, D-JNKI1 inhibited APP phosphorylation in Thr-668 and reduced the amyloidogenic cleavage of APP and A $\beta$  oligomers in brain parenchyma of treated mice. In conclusion, by regulating key pathogenic mechanisms of AD, JNK might hold promise as innovative therapeutic target.

Alzheimer disease (AD)<sup>3</sup> is a progressive neurodegenerative disorder that begins with episodic short term memory deficits (1) and culminates with long term memory impairment and total loss of cognitive functions. A growing body of evidence shows that A $\beta$

peptides and their soluble intermediates A $\beta$  oligomers (2), which derive from the processing of amyloid precursor protein (APP) are the primary toxic agents in AD (3–6). A $\beta$  oligomers induce the synaptic failure or dysfunction of the excitatory synaptic button (3, 7, 8) associated with memory dysfunction (9, 10). Elucidating the intracellular signaling pathway that regulates the neurodegenerative stages of AD will offer the chance to interfere with these key players and revert or at least slow down disease progress. One pathway that may be involved in AD pathogenesis is JNK.

The JNK signaling pathway is activated in human AD brains (11, 12) also at early disease stages (11). Furthermore, the JNK pathway can be triggered by A $\beta$  peptides (13), and it mediates A $\beta$ -induced long term potentiation (LTP) deficit in hippocampal slices (14). JNK phosphorylates the APP (15–17) leading to an increase in A $\beta$  fragment levels *in vitro* (18) and plays a role in Tau phosphorylation (19–21), thus linking to another important hallmark of the disease. Finally, a recent study suggested a critical involvement of JNK in stress-induced modulation of memory (22). In view of the above, JNK surely represents an intriguing cross-road in AD.

To determine the role of JNK in AD pathogenesis its specific inhibition should be tested in an *in vivo* model that mimics AD. In this study, we provide a first report of chronic JNK inhibition in TgCRND8 mice. JNK inhibition was achieved by treating TgCRND8 mice with the cell-penetrating inhibitor peptide, D-JNKI1 (23, 24), which, to date, represents the most specific JNK inhibitor available.

We showed for the first time that chronic treatment with D-JNKI1 rescues cognitive dysfunction, memory impairment, and LTP in TgCRND8 mice. Moreover, it modulates APP processing leading to inhibition of toxic soluble A $\beta$  production without any major side effects.

## EXPERIMENTAL PROCEDURES

Experimental procedures on animals were conducted in accordance with the European Communities Council Directive

\* This work was supported by Marie Curie Industry-Academia Partnerships and Pathways Cpads (to T. B.), San Paolo 2008-2437 (to T. B.), Cassa di Risparmio delle Provincie Lombarde (CARIPLO) 2009-2425 (to T. B.), and Swiss National Foundation (SNF) Grant 310030\_130500 (to G. G. C.).

[5] The on-line version of this article (available at <http://www.jbc.org>) contains supplemental Fig. 1.

<sup>1</sup> Both authors contributed equally to this work.

<sup>2</sup> To whom correspondence should be addressed: Neuronal Death and Neuroprotection Lab., Dept. of Neuroscience, Istituto Di Ricerche Farmacologiche "Mario Negri," Via la Masa 19, 20156 Milano, Italy. Tel.: 39-02-39014469; Fax: 39-02-39001916; E-mail: tiziana.borsello@marionegri.it.

<sup>3</sup> The abbreviations used are: AD, Alzheimer disease; ACSF, artificial cerebrospinal fluid; APP, amyloid precursor protein; fEPSP, field excitatory postsynaptic potential; ANOVA, analysis of variance; D.I., discrimination index; LTP, long term potentiation; Tg, transgenic.

## JNK Inhibition Prevents AD

(86/609/EEC) and were authorized by Italian legal guidelines. All efforts were made to minimize the number of animals used and their suffering.

**Transgenic Mice and Pharmacological Treatments**—TgCRND8 mice (25) were housed at 23 °C room temperature with food and water *ad libitum* and a 12-h light/dark cycle. TgCRND8 mice were treated chronically with D-JNK11 (Mario Negri Institute for Pharmacological Research) diluted in water (22 mg/kg) or with water as vehicle starting at 4–5 months of age. Mice received an intraperitoneal injection every 21 days for 5 months (six injections). For the acute treatment, animals received one injection with vehicle or D-JNK11 (11 mg/kg or 22 mg/kg) and were sacrificed after 3 weeks. D-TAT (Mario Negri Institute for Pharmacological Research) was used as control for the electrophysiological tests.

**Novel Object Recognition Test and Open Field**—The effect of D-JNK11 treatment on memory was tested on TgCRND8 and WT mice using the object recognition task. Animals were randomized into four groups: WT vehicle, WT D-JNK11 Tg vehicle, and Tg D-JNK11 treated mice. For the 3-day test, mice were placed in an open-square arena with the floor divided into 25 squares by black lines. The first day (open field) animals were placed in the empty arena for 5 min, and the number of line crossings was recorded. The second day mice were exposed to two identical objects. A black plastic cylinder, a glass vial, and a metal cube were used. Exploration was recorded in a 10-min trial. The third day, mice were replaced in the arena containing one familiar object and a novel object, different from the familiar one. Time spent exploring the two objects was recorded on video in a 10-min trial and analyzed by an investigator blinded to the strain and treatment. Memory was expressed as a discrimination index (D.I.), *i.e.* (seconds on novel seconds on familiar)/(total seconds on objects).

**Eight-arm Radial Maze**—Spatial working memory was measured using an eight-arm radial maze, with each arm radiating from an octagonal central arena containing 50  $\mu$ l of water at the end. Several extra maze visual cues were positioned around the apparatus. Water deprivation started 1 week before the task (water available for 1 h/day for the duration of the training). One day before starting the task, a 10-min habituation trial was run. The next day, the animals were placed in the center of the maze, and the arm-entry sequence was recorded. The task ended once all eight arms had been visited or after a maximum of 16 trials, whichever came first. Repeated entries into an arm previously visited constituted an error. The numbers of correct entries, errors, and the latency to complete the test were recorded manually.

**Electrophysiology**—Mice were decapitated, and the brain was removed and immersed for 2–3 min in ice-cold artificial cerebrospinal fluid (ACSF) containing the following: 126 mM NaCl, 2.5 mM KCl, 1.2 mM MgCl<sub>2</sub>, 1.2 mM NaH<sub>2</sub>PO<sub>4</sub>, 2.4 mM CaCl<sub>2</sub>, 10 mM glucose, and 25 mM NaHCO<sub>3</sub>, continuously bubbled with 95% O<sub>2</sub> and 5% CO<sub>2</sub>, pH 7.4. The hippocampus was extracted and cut in ice-cold ACSF with a vibratome (Pelco 1000 plus; Redding, CA) into 400- $\mu$ m thick transverse slices, which were allowed to recover in oxygenated ACSF at 30 °C for 30 min, and then at room temperature for another 1–2 h before experimental recordings. A slice was transferred into the recording cham-

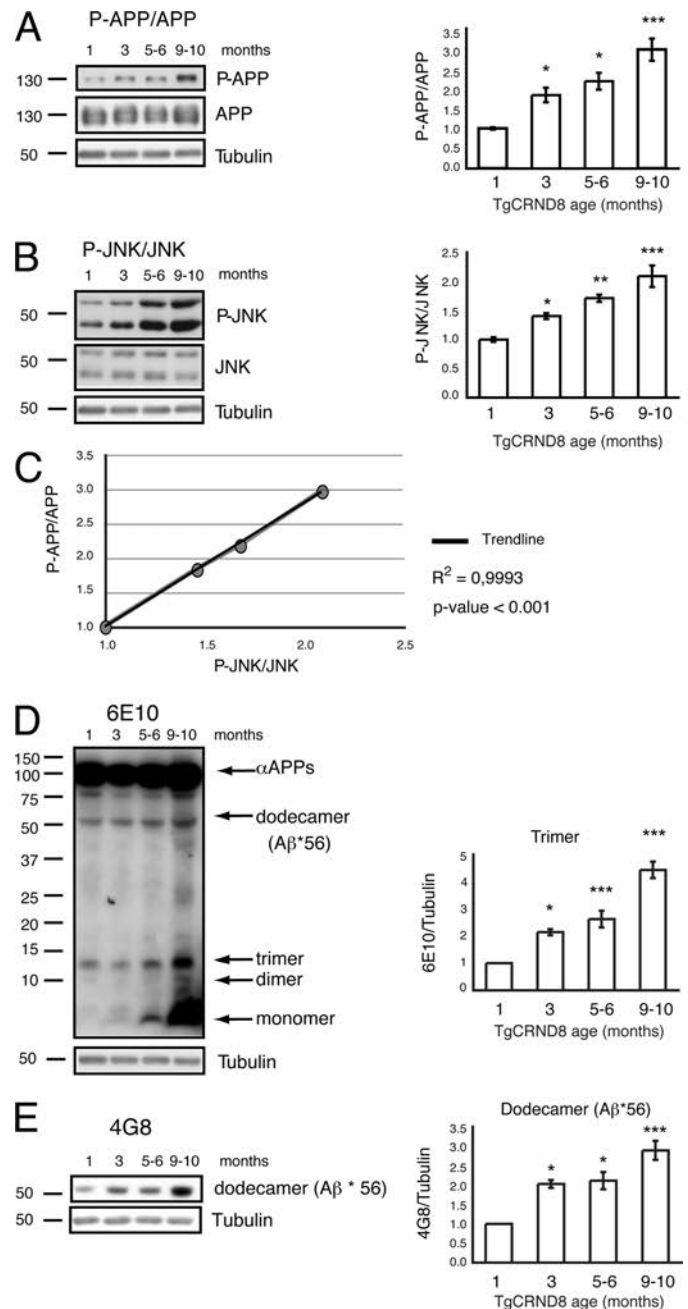


**FIGURE 1. JNK activation correlates with an increase in APP<sub>Thr-668</sub> phosphorylation and A $\beta$  oligomers in TgCRND8 mice.** A, p-APP/APP levels increased with disease progression in TgCRND8 mice as shown by the representative Western blot and relative quantification. Data are expressed as mean  $\pm$  S.E. (one-way ANOVA). \*,  $p < 0.05$ ; \*\*\*,  $p < 0.001$  versus 1 month ( $n = 8$ ); Dunnett's post hoc test. B, p-JNK levels increased with disease progression in TgCRND8 mice as shown by the representative Western blot and relative quantification. Data are expressed as mean  $\pm$  S.E. (one-way ANOVA). \*,  $p < 0.05$ ; \*\*,  $p < 0.01$ ; \*\*\*,  $p < 0.001$  versus 1 month ( $n = 8$ ); Dunnett's post hoc test. C, correlation curve of p-APP and p-JNK in TgCRND8 mice at different time points are indicated by the black circles ( $R^2 = 0.9993$ ;  $p < 0.001$ ). D, representative Western blot showing the formation of toxic soluble A $\beta$  forms (dimers, trimers) with increasing age in TgCRND8 mice. Bar graphs show densitometric analysis of Western blots. Data are expressed as mean  $\pm$  S.E. (one-way ANOVA). \*,  $p < 0.05$ ; \*\*\*,  $p < 0.001$  versus 1 month ( $n = 8$ ); Dunnett's post hoc test. E, increased formation of dodecamer with increasing age was detected in TgCRND8 mice by Western blotting. Bar graphs show densitometric analysis of Western blots. Data are expressed as mean  $\pm$  S.E. (one-way ANOVA). \*,  $p < 0.05$ ; \*\*\*,  $p < 0.001$  versus 1 month ( $n = 8$ ); Dunnett's post hoc test.

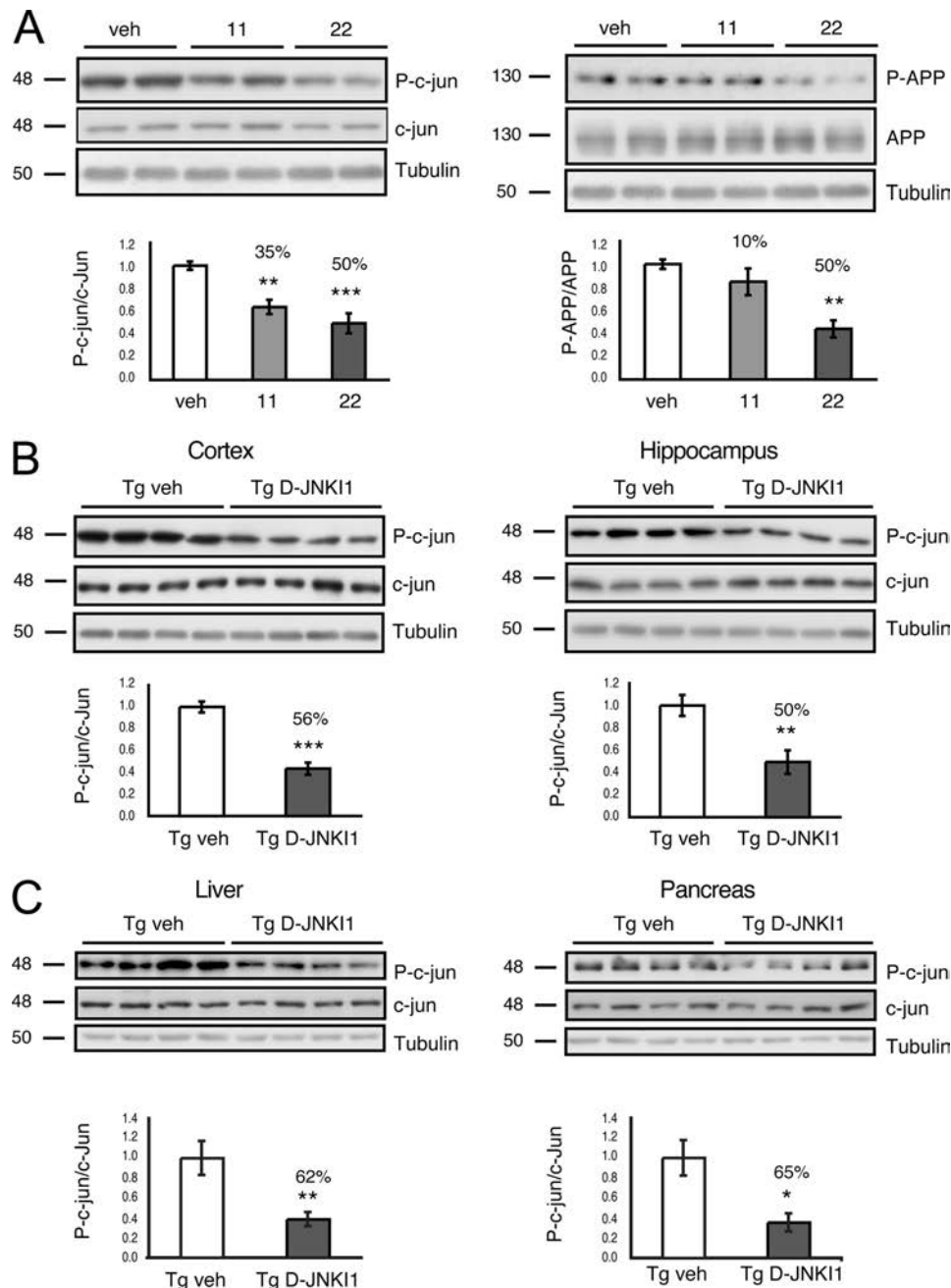


**FIGURE 2. Treatment with D-JNK11 inhibits phosphorylation of c-Jun and APP.** A, representative Western blots and relative quantifications show that increasing doses of D-JNK11 inhibit phosphorylation of c-Jun by 35 and 50%, respectively. 22 mg/kg of D-JNK11 inhibits phosphorylation of APP by 50%. Data are expressed as mean  $\pm$  S.E. (one-way ANOVA). \*\*,  $p < 0.01$ ; \*\*\*,  $p < 0.001$  versus vehicle (veh) ( $n = 6$ ); Dunnett's post hoc test. B, chronic treatment with D-JNK11 in TgCRND8 leads to a 56 and 50% decrease in phosphorylation of c-Jun in the cortex and hippocampus, respectively. Data are expressed as mean  $\pm$  S.E. \*\*,  $p < 0.01$ ; \*\*\*,  $p < 0.001$  (Tg vehicle ( $n = 8$ ) versus Tg D-JNK11 ( $n = 8$ ); Student's  $t$  test). C, Western blots and relative quantifications showing that chronic treatment with D-JNK11 in TgCRND8 leads to a 62 and 65% decrease in phosphorylation of c-Jun in the liver and pancreas, respectively. Data are expressed as mean  $\pm$  S.E. \*,  $p < 0.05$ ; \*\*,  $p < 0.01$  (Tg vehicle ( $n = 8$ ) versus Tg D-JNK11 ( $n = 8$ ); Student's  $t$  test).

ber and submerged in ACSF at a constant rate of 2.5 ml/min at 30 °C. Recording electrodes were made of borosilicate glass capillaries (GC150F-10; Harvard Apparatus) and filled with 2 M NaCl (resistance, 10–15 megaohms).

Under visual control, the stimulating electrode was inserted into the Schaffer collateral fibers, and the recording electrode was inserted into the CA1 region. Testing stimuli of 0.1 Hz, 10  $\mu$ s duration, and 20–30 V amplitude evoked field EPSPs, which were 50–70% of maximum slope. fEPSPs were filtered at 3 KHz,

digitized at 10 KHz, and stored on a personal computer. An Axoclamp 2B amplifier (Axon Instruments) was used for extracellular recordings. After recording a stable baseline for 20 min, LTP was induced by high frequency stimulation consisting of a 1-s train at 100 Hz at a stimulus strength corresponding to 70% of maximum response. The initial slope of the response was used to assess changes in synaptic strength.

**Sample Collection**—Animals were perfused transcardially with ice-cold PBS (Invitrogen-Invitrogen), and brains were col-

## JNK Inhibition Prevents AD

lected and divided in the two hemispheres. Left hemispheres were then fixed in 4% paraformaldehyde, dehydrated for 24 h in 20–30% sucrose in PBS, and frozen in *N*-pentane for histology; right hemispheres were homogenized in 1% Triton X-100 lysis buffer supplemented with proteases (1× complete protease inhibitor cocktail, CPIC, Roche) and phosphatases (1 μM 4-nitrophenyl phosphate 4-NPP, Roche) inhibitors (24) and used for Western blot. Soluble fractions were prepared by centrifuging the total homogenate at 100,000 × *g* for 45 min; the supernatant was collected and used for Western blot analysis of sAPPα and sAPPβ soluble fragments. Peripheral tissues (liver and pancreas) were additionally collected and homogenized in the same buffer for Western blot analysis.

**Western Blot**—Proteins were separated by 10% SDS-polyacrylamide gel and transferred to a PVDF membrane. C-83/C-99 fragments and Aβ species labeled with 6E10 and 4G8 were separated by gradient NuPAGE Novex Bis-Tris Mini Gels System (Invitrogen-Invitrogen). All blots were normalized to α-tubulin. Western blots were quantified using ImageQuant TL software (Amersham Biosciences).

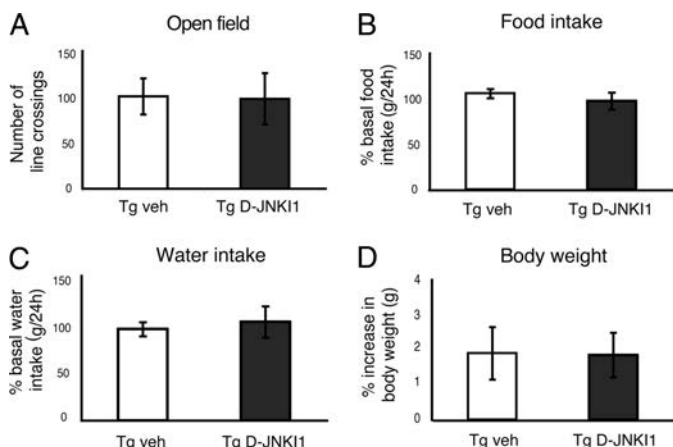


**FIGURE 3. Chronic treatment with D-JNK11 does not lead to any major side effects.** *A*, locomotor activity in the open field test was similar for vehicle (*veh*) and D-JNK11-treated mice,  $p = 0.937$  (Tg vehicle ( $n = 8$ ) versus Tg D-JNK11 ( $n = 8$ ); Student's *t* test). *B* and *C*, chronic treatment with D-JNK11 had no effects on food and water intake,  $p = 0.446$  (food) (Tg vehicle ( $n = 8$ ) versus Tg D-JNK11 ( $n = 8$ );  $p = 0.672$  (water) (Tg vehicle ( $n = 8$ ) versus Tg D-JNK11 ( $n = 8$ ); Student's *t* test). Data are expressed as the ratio between food and water consumption in the 24 h before D-JNK11 treatment to that after each D-JNK11 injections. *D*, no difference in the body weight gain in Tg mice was found during the five months of D-JNK11 treatment ( $p = 0.96$  (Tg vehicle ( $n = 8$ ) versus Tg D-JNK11 ( $n = 8$ ); Student's *t* test). Data are expressed as mean ± S.E.

**TABLE 1**

**Analysis of major toxicological markers in plasma demonstrates that D-JNK11 chronic treatment does not lead to any major side effects in mice**

Data are expressed as mean (S.E.) (two-way ANOVA); NS, not significant.

	WT vehicle	WT D-JNK1	Tg vehicle	Tg D-JNK1	Two-way ANOVA
Number	6	4	6	4	
Bilirubin total (μmol/liter)	0.110 (0.031)	0.143 (0.091)	0.128 (0.026)	0.065 (0.019)	NS
Calcium (μmol/liter)	2.192 (0.109)	2.468 (0.107)	2.354 (0.079)	2.430 (0.099)	NS
Creatinine (μmol/liter)	0.268 (0.011)	0.285 (0.009)	0.272 (0.005)	0.285 (0.017)	NS
Glutamylxaloacetic transaminase (units/liter)	187.3 (96.600)	194.4 (74.114)	111.8 (21.086)	130.6 (32.363)	NS
Glutamylpyruvic transaminase (units/liter)	88.6 (53.272)	58.4 (16.703)	28.9 (7.101)	35.6 (7.454)	NS
Urea (mmol/liter)	34.2 (2.873)	45.8 (2.406)	51.2 (2.160)	60.1 (6.360)	NS
α-Amylase (units/liter)	2673.3 (141.270)	3134.7 (200.073)	2704.5 (170.604)	2744.8 (297.337)	NS
Alkaline phosphatase (units/liter)	106.4 (15.836)	75.5 (9.805)	85.2 (12.065)	85.0 (7.524)	NS
Lactate dehydrogenase (units/liter)	442.5 (165.561)	395.8 (71.976)	264.9 (34.254)	379.0 (60.603)	NS
Sodium (mmol/liter)	162.4 (2.401)	156.9 (1.165)	160.0 (2.988)	164.3 (1.971)	NS
Potassium (mmol/liter)	6.578 (0.218)	7.107 (0.462)	7.314 (0.460)	6.90 (0.398)	NS
Chlorine (mmol/liter)	112.3 (1.192)	111.6 (4.148)	111.2 (1.623)	115.1 (0.971)	NS

**Histology**—Slices of frozen tissue 30-μm-thick were cut on a cryostat. The slices were incubated with 1% H<sub>2</sub>O<sub>2</sub> for 5 min, blocked for 1 h with 10% normal goat serum, and incubated overnight with 4G8 antibody. After exposure to secondary biotinylated goat anti-mouse antibody, ABC solution (Vector Laboratories) was added, followed by application of 3'-3'-diaminobenzidine (Sigma Aldrich). Images were acquired with Analysis software (Olympus). The total plaques area per slice was quantified using ImageJ software.

**Antibodies**—The following primary antibodies were used: antibody to APP clone 22C11 (1:2000, Chemicon), p-APP (1:500, a generous gift from Professor P. Davis, Albert Einstein College of Medicine of Yeshiva University), p-c-Jun (1:1000, Cell Signaling Technology), c-Jun (1:1000, Cell Signaling Technology), APP C-terminal (1:2000, Sigma Aldrich), αAPPs (6E10, 1:1000, Abcam), βAPPs (1:1000, IBL-America), β-amyloid (6E10, 1:1000, Abcam; 4G8, 1:2000, Signet), α-tubulin (Santa Cruz Biotechnology), and A11 antibody (1:1000, Invitrogen). 4G8 monoclonal antibody (1:250) was used to visualize senile plaques on brain sections.

**Side Effect Screening**—The body weight of TgCRND8 and WT mice was recorded throughout the experiment. The net gain was calculated for each mouse and taken as an indicator of growth during the five months of treatment. The effects of D-JNK11 on food and water consumption were calculated as the ratio of the intake in the 24 h after each D-JNK11 treatment to consumption in the 24 h before each treatment.

**Necropsy**—Vehicle and D-JNK11 animals were sacrificed with high CO<sub>2</sub> concentrations and were examined for macroscopic lesions on the main organs. Liver, kidney, and digestive organs were fixed in formalin for histopathological analysis.

**Toxicological Analysis**—Toxicological analysis was performed using a Beckman Coulter AU480 analyzer (Beckman Coulter, Krefeld, Germany). The AU480 is an automated chemistry instrument for turbidimetric, spectrophotometric, and ion-selective electrode measurements. Briefly, 110 μl of plasma in 1.5-ml Eppendorf tubes was used to measure sodium, potassium, chloride, calcium, creatinine, urea, α-amylase, aspartate aminotransferase, alanine aminotransferase, alkaline phosphatase, lactate dehydrogenase, and total bilirubine according to the manufacturer's protocol.

**Statistical Analysis**—Statistical analysis was done using StatView software. Data were calculated as mean ± S.E. Differences between groups were compared using Student's *t* test or one-

way ANOVA and two-way ANOVA followed by Dunnett or Tukey's test. *p* values < 0.05 were considered significant.

**RESULTS**

**Characterization of Model**—Phosphorylation of APP at Thr-668 in the brain of TgCRND8 mice was assessed by Western

blotting; p-APP/APP ratio increased with increasing age (Fig. 1A, p-APP/APP and its densitometry quantification). In a similar manner, phosphorylation of JNK progressively augmented starting from the third month of age (Fig. 1B, p-JNK/JNK ratio with quantification) and correlated with phosphorylation of APP (see correlation curve in Fig. 1C).

Aβ-soluble forms in TgCRND8 brains were assessed by Western blotting to link Aβ toxic species to AD-related memory deficits that in our model appear already by the third month of age (26, 27). Toxic soluble Aβ forms (dimers, trimers) were detected in TgCRND8 parenchyma with the 6E10 antibody, which is more specific for lower Aβ forms (5), and the 4G8 antibody, which is more specific for higher species (dodecamer). Monomer, dimer, and trimer Aβ species were increased by the third month of age. A further increase was observed with disease progression (4–10-month-old mice) (Fig. 1, D and E). The A11-positive Aβ dodecamer (5) (referred to as Aβ\*56, see supplemental Fig. 1) was also present at three months and followed the trend of the lower Aβ forms (Fig. 1, D and E).

**D-JNK11 Inhibits Both c-Jun and Phospho APP<sub>Thr-668</sub> in Dose-dependent Manner in TgCRND8 Mice**—The ability of D-JNK11 to chronically inhibit phosphorylation of c-Jun and APP on Thr-668 *in vivo* was assessed by Western blotting in both the cortex and hippocampus (Fig. 2A).

Administration of increasing doses of D-JNK11 (11 mg/kg and 22 mg/kg) led to a dose-dependent decrease in the phosphorylation of c-Jun, whereas scrambled control peptide had no effect (see previous work, Ref. 23). Differently, inhibition of APP phosphorylation was achieved only with higher D-JNK11 dosages.

**Chronic Treatment with D-JNK11 Inhibits p-c-Jun without Leading to Side Effects in TgCRND8 Mice**—D-JNK11 (22 mg/kg) was injected intraperitoneally every 3 weeks for a period of 5 months to chronically prevent JNK action *in vivo*. The efficiency of D-JNK11 treatment on the phosphorylation of c-Jun in the brain as well as in two peripheral tissues, liver and pancreas, was assessed by Western blotting. D-JNK11 inhibited the phosphorylation of c-Jun both in the cortex and hippocampus by 56 and 50%, respectively (Fig. 2B). In a similar manner, phos-

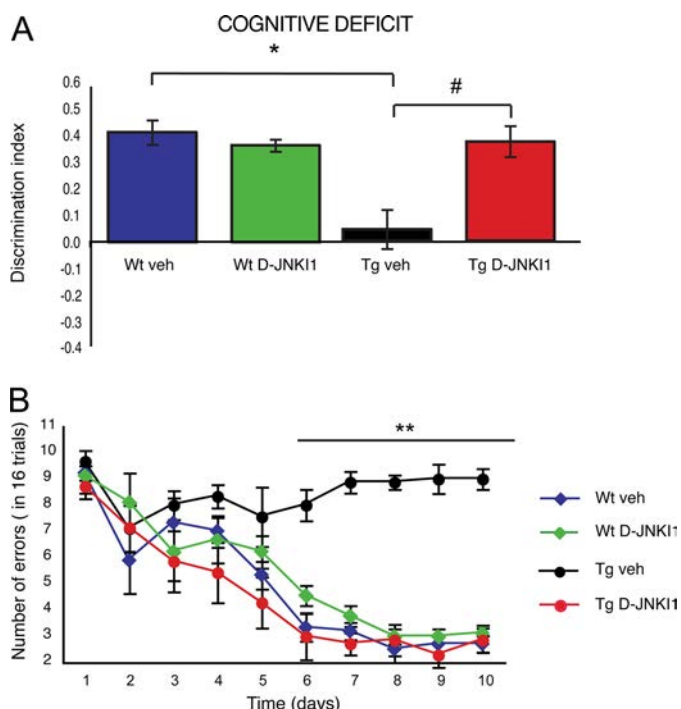


**FIGURE 4. Treatment with D-JNK11 reverses memory deficits.** A, object recognition test. WT animals treated with either vehicle (WT veh; *n* = 9) or D-JNK11 (WT DJNK11; *n* = 10) had no memory impairment (D.I. = 0.42 and 0.37, respectively). Vehicle-treated Tg mice (Tg veh; *n* = 10) had significant memory impairment (D.I. = 0.043) compared with WT vehicle mice. In Tg mice (Tg DJNK11; *n* = 7) D-JNK11 fully rescued memory deficit (D.I. = 0.38) (two-way ANOVA). \*, *p* < 0.05 WT+vehicle versus Tg+vehicle; #, *p* < 0.05 Tg vehicle versus Tg+D-JNK11; Tukey's post hoc test. B, eight-arm radial maze. Unlike vehicle-treated WT mice (WT veh; *n* = 9), vehicle-treated Tg mice (Tg veh; *n* = 10) did not improve their performance during training, as showed by the high number of errors per day. D-JNK11 treated mice (Tg DJNK11; *n* = 7) significantly improved their performance, overlapping that of control mice (WT vehicle). D-JNK11 induced no deficit in WT mice (WT DJNK11; *n* = 10). Data are expressed as mean ± S.E. (two-way ANOVA). \*\*, *p* < 0.01 WT+vehicle, WT+D-JNK11, and Tg+D-JNK11 versus Tg vehicle (Tukey's post hoc test).

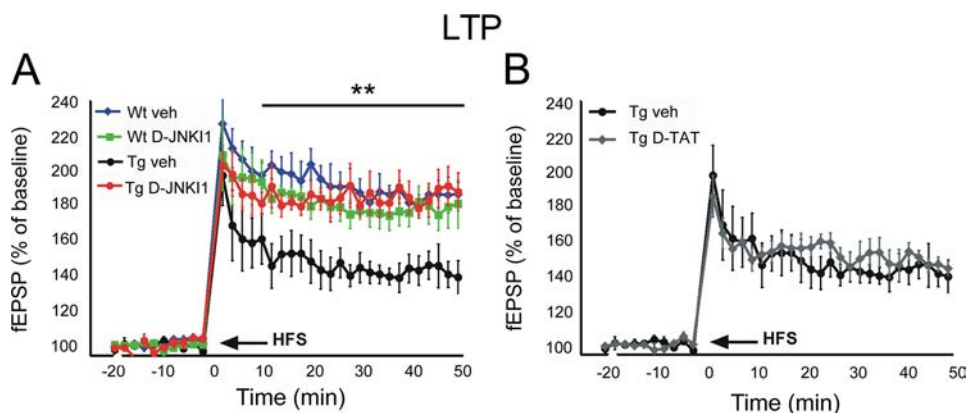
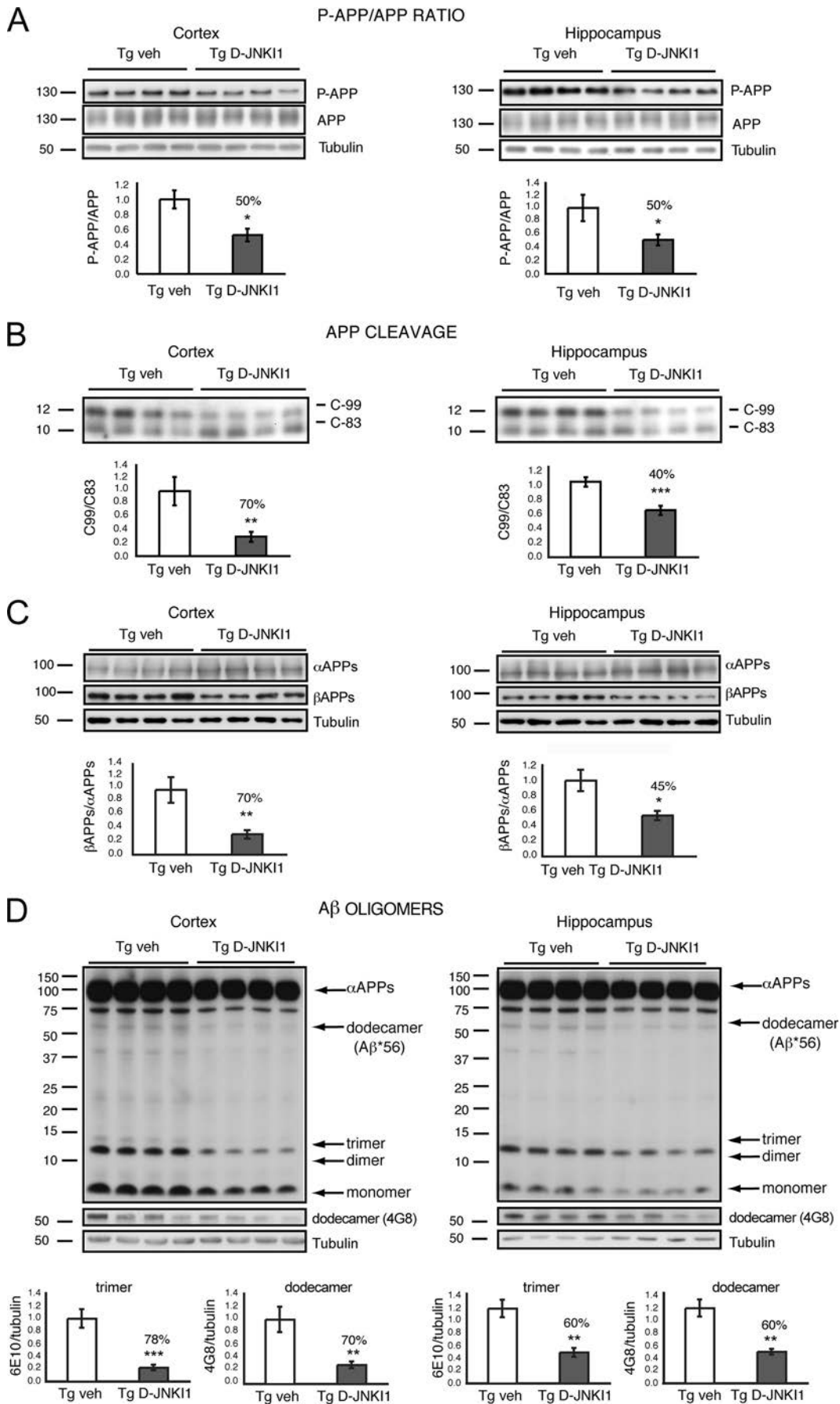


**FIGURE 5. Treatment with D-JNK11 reverses LTP impairment.** Graphs showing LTP of fEPSP slope in hippocampal slices from TgCRND8 mice. A, LTP in Tg vehicle mice (*n* = 9), was smaller than that in WT vehicle mice (*n* = 10). LTP of Tg mice treated with D-JNK11 (*n* = 13) was superimposed to that of WT vehicle (veh) mice. D-JNK11 did not affect LTP in WT mice (WT DJNK11; *n* = 14) (two-way ANOVA). (interaction, *p* < 0.001, \*\*, *p* < 0.01, WT+vehicle, WT+D-JNK11, and Tg+D-JNK11 versus Tg vehicle; Tukey's post hoc test). B, D-TAT alone was used as inactive control peptide and did not affect LTP of Tg mice (*n* = 12). fEPSP curves of Tg mice treated with vehicle or D-TAT were superimposed. Data are expressed as mean ± S.E.; *n* is the number of slices.



phorylation of c-Jun was inhibited by 62% in the liver and 65% in the pancreas (Fig. 2C), indicating that D-JNK11 can inhibit phosphorylation of c-Jun in the brain almost as efficiently as in peripheral tissues.

As this is the first time that D-JNK11 was administered chronically, it was important to test whether chronic D-JNK11 treatment elicited any toxic side effects. We first examined open field activity, food and water intake, and body weight of Tg D-JNK11 mice as indexes of their general health status (Fig. 3, A–D). Compared with Tg vehicle mice, D-JNK11 treatment did not affect mice survival. Tg D-JNK11 mice behaved normally in the open field test (Fig. 3A) and had normal food and water intake (Fig. 3, B and C) as well as body weight (Fig. 3D).

A more in-depth toxicological analysis was subsequently carried out. Liver, kidney, and pancreas markers as well as hemolysis and ion levels were tested in whole blood from D-JNK11 and vehicle-treated mice. No significant differences were detected between D-JNK11 and vehicle-treated WT or Tg mice in any of the parameters analyzed (Table 1), indicating lack of toxicity by chronic D-JNK11 treatment.

Moreover, upon necropsy, no tumors were detected in lung, skin, or liver. Therefore, D-JNK11 chronic treatment does not lead to any major side effects, neither due to cell-permeable peptides (arginine-rich peptide) nor due to partial inhibition of JNK action.

**D-JNK11 Rescues Cognitive Deficits in TgCRND8 Mice**—To determine the importance of JNK in AD pathology, D-JNK11 treatment was commenced at 4–5 months of age, and thus when toxic A $\beta$  forms and plaque accumulation are already present. The ability of D-JNK11 to rescue impaired cognitive functions was tested by measuring memory impairment with two behavioral tasks: novel object recognition test and radial maze.

Hippocampal function was investigated by the novel object recognition test, a non-invasive task that relies on the mouse natural exploratory behavior. Open field study showed that WT vehicle, WT D-JNK11, Tg vehicle, and Tg D-JNK11 mice had no deficits in habituation and locomotion in novel environments. During the training section, the mice spent the same amount of time exploring the two objects. The following day, when a novel object was introduced, vehicle and WT D-JNK11 mice performed well and distinguished familiar from novel objects, whereas Tg vehicle mice had a significantly lower D.I., confirming the impaired memory (Fig. 4A). In contrast, Tg D-JNK11 mice spent more time on novel objects and behaved similarly to WT mice. Thus, D-JNK11 rescued hippocampal function in Tg mice.

To support this finding, we also evaluated the effect of D-JNK11 in the eight-arm radial maze, a selective spatial work-

ing memory task (28, 29). All four groups (WT vehicle, WT D-JNK11, Tg vehicle, and Tg D-JNK11) were trained until they met the criterion of fewer than two errors on three consecutive days. The performance of Tg mice was below that of WT; thus, the cognitive deficit of Tg mice was evident. As shown in Fig. 4B, Tg vehicle mice did not improve their performance for the whole duration of the trial, proving that Tg mice have cognitive deficits in working memory compared with WT mice (Fig. 4B) (30). In contrast, Tg D-JNK11 mice presented a progressive daily improvement in performance, indicating that they were still able to learn. There were no differences between the vehicle-treated and the D-JNK11-treated WT animals. These results provide evidence that JNK inhibition prevented long term memory impairment as well as the dysfunction of working memory and recall in TgCRND8 mice.

**D-JNK11 Regulates Synaptic Dysfunction in TgCRND8 Mice**—To test whether D-JNK11 is able to impact on synaptic dysfunction, we assessed hippocampal LTP, one of the main paradigms for measuring long lasting changes in synaptic plasticity (31), by electrophysiological tests.

LTP produced by a conditioning protocol in the CA1 region was tested in five groups: wild-type mice (WT vehicle), WT mice treated with D-JNK11 (WT D-JNK11), TgCRND8 mice (Tg vehicle), TgCRND8 mice treated with D-JNK11 (Tg D-JNK11), and TgCRND8 treated with an inactive control peptide (Tg TAT) (Fig. 5). As shown in Fig. 5A, transgenic mice had a considerably smaller LTP than WT mice, whereas the fEPSP of Tg D-JNK11 mice returned to control values. The effect of D-JNK11 was specific since the inactive peptide (D-TAT) did not affect LTP of Tg mice (Fig. 5B). These results demonstrate that the specific inhibition of JNK with D-JNK11 completely rescues the LTP deficit in TgCRND8 and emphasizes the importance of JNK signal transduction in regulating synaptic plasticity during the pathological events.

**JNK Regulates Pathological Form of A $\beta$  in TgCRND8 Mouse Brains**—Because the accumulation of A $\beta$  peptides, derived via APP processing, is responsible for memory decline as well as for synaptic dysfunction (3, 7, 8, 32), we investigated the effect of D-JNK11 in TgCRND8 mice focusing on the processing of APP<sup>Sw/In</sup> linked to familial AD. D-JNK11 prevented APP phosphorylation at Thr-668 *in vivo* and reduced the p-APP/APP ratio by 50% in the cortex and the hippocampus of TgCRND8 mice as compared with vehicle-treated ones (Fig. 6A).

To further analyze the effect of D-JNK11 on amyloidogenic APP processing, APP cleavage was examined by assessing the ratio of C-99 to C-83 fragments by Western blotting. As displayed in Fig. 5B, D-JNK11 reduced C-99 levels and raised C-83 levels, resulting in a drop of the C-99/C-83 ratio by 70% in the cortex and 40% in the hippocampus (Fig. 6B).

**FIGURE 6. D-JNK11' effect on APP processing.** A, p-APP/APP ratio. Representative Western blot and relative quantification showed that the p-APP/total APP ratio is reduced in the cortex and hippocampus of Tg DJNK11 mice compared with controls. Data are expressed as mean  $\pm$  S.E. \*,  $p < 0.05$  (Tg vehicle ( $n = 8$ ) versus Tg D-JNK11 ( $n = 8$ ); Student's  $t$  test). B, APP fragments Western blots and relative quantifications. The C-99/C-83 ratio was reduced by 70% in the cortex and 40% in the hippocampus of Tg D-JNK11 mice compared with controls. Data are expressed as mean  $\pm$  S.E. \*\*,  $p < 0.01$ ; \*\*\*,  $p < 0.001$  (Tg vehicle ( $n = 8$ ) versus Tg D-JNK11 ( $n = 8$ ); Student's  $t$  test). C, soluble  $\alpha$ APP and  $\beta$ APP Western blots and relative quantifications.  $\beta$ APP/ $\alpha$ APP ratio was reduced by 70% in the cortex and 45% in the hippocampus of Tg DJNK11 mice. Data are expressed as mean  $\pm$  S.E. \*,  $p < 0.05$ ; \*\*,  $p < 0.01$  (Tg vehicle ( $n = 8$ ) versus Tg D-JNK11 ( $n = 8$ ); Student's  $t$  test). D, Western blots and relative quantifications. Formation of toxic soluble A $\beta$  trimers is reduced by 78% and of dodecamers by 70% in the cortex of Tg D-JNK11-treated mice. Formation of toxic soluble A $\beta$  trimers is reduced by 60% and of dodecamers by 60% in the hippocampus of Tg D-JNK11 treated mice. Data are expressed as mean  $\pm$  S.E. \*\*,  $p < 0.01$ ; \*\*\*,  $p < 0.001$  (Tg vehicle (veh;  $n = 8$ ) versus Tg D-JNK11 ( $n = 8$ ); Student's  $t$  test).

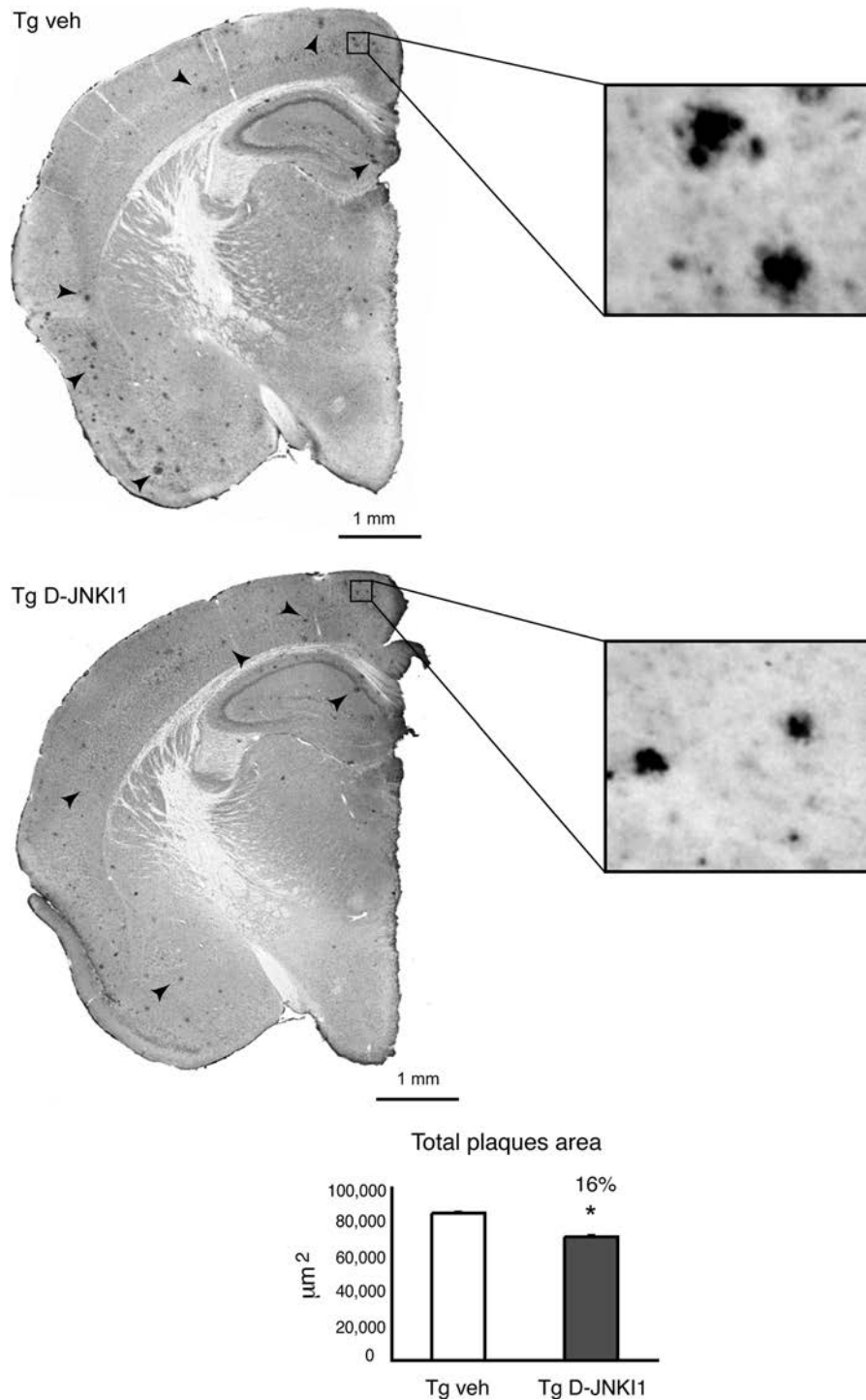


FIGURE 7. D-JNK11 treatment decreases plaques formation. Representative brain slices were stained with 4G8 to visualize A $\beta$  plaques. Higher magnification demonstrated a clear reduction in the total area of plaques. As shown in the graph at 9–10 months of age total area of the plaques was decreased in Tg D-JNK11 mice by 16% compared with Tg vehicle (*veh*). Data are expressed as mean  $\pm$  S.E. \*,  $p < 0.05$  (Tg vehicle ( $n = 8$ ) versus Tg D-JNK11 ( $n = 8$ ); Student's *t* test).

We further investigated the D-JNK11 effect on APP cleavage by analyzing  $\alpha$ APP and  $\beta$ APP metabolites in the soluble fractions. Expression of  $\alpha$ APPs increased by 1.8-fold, whereas  $\beta$ APPs decreased by 50% (data not shown) in D-JNK11-treated mice compared with Tg vehicle mice. The ratio between the soluble fragments was reduced by 70% (Fig. 6C), consistent with the data on APP processing (Fig. 6B). Instead, in the hippocampus,  $\alpha$ APP fragments increased, although not significantly,

whereas  $\beta$ APPs decreased by 33% (data not shown). The  $\beta$ APP/ $\alpha$ APP ratio was decreased by 45% (Fig. 6C), confirming the data with the C-terminal fragments (Fig. 6B). Thus, *in vivo*, D-JNK11 prevents the amyloidogenic  $\beta$ APP formation and favors  $\alpha$ -secretase cleavage by inhibition of APP phosphorylation.

To test whether D-JNK11 is able to decrease circulating A $\beta$ -soluble oligomers in the brain parenchyma, we performed Western blot analysis using the antibodies 6E10 and 4G8,

which specifically recognize the more toxic A $\beta$  trimers and dodecamers, respectively. Both trimers and dodecamers were reduced by 78 and 70%, respectively, in the cortex of Tg D-JNK11 mice (Fig. 6D). Similarly, in the hippocampus of Tg D-JNK11 mice, both trimers and dodecamers were reduced by 60% (Fig. 6D). Thus, in TgCRND8 mice, D-JNK11 is efficient in shifting the APP to non-amyloidogenic processing, and it inhibits A $\beta$  oligomer formation, responsible of synaptic dysfunction and loss.

**D-JNK11 Treatment Diminishes Plaque Formation**—Brains of 9–10-month-old mice were processed to determine the effect of the peptide on A $\beta$  plaque deposition (Fig. 7). Treatment with D-JNK11 reduced plaque formation by 16% compared with vehicle-treated Tg mice (Fig. 7).

## DISCUSSION

TgCRND8 mice are a well characterized murine model that mimic AD because they reproduce important features of the disease: cognitive deficits, amyloid plaques (33), and hyperphosphorylation of Tau (34). We showed that phosphorylation of APP<sub>Thr-668</sub> (16, 35–38) as well as production of A $\beta$  toxic species is augmented by the third month of age, a finding that correlates with an increase in JNK activation. Accordingly, the activation of JNK pathway has been reported in the Tg2576 and Tg2576/PS1<sup>P264L</sup> preclinical models of AD (39, 40).

D-JNK11 represents a unique tool to study the JNK signaling pathway and to perform a chronic treatment *in vivo*. This peptide prevents exclusively the action of JNK on its JNK binding domain (JBD)-dependent targets, resulting in a partial inhibition of the enzyme that is nevertheless activated and thus able to phosphorylate JBD-independent targets (41). D-JNK11 crosses the blood-brain barrier successfully (19, 23, 42), it is composed of D-amino acids that are not easily degraded by proteases and is not immunogenic (D-amino acid form is not recognized).

We have previously shown that a dose of 11 mg/kg is neuroprotective against stroke (acute injury) (23). In treating TgCRND8 mice (chronic injury), we increased the dose to 22 mg/kg, which was required to decrease the p-APP/APP ratio.

Additionally, D-JNK11 treatment does not lead to any apparent side effects. These results point to the potential use of a peptide that prevents JNK action as a new therapeutic strategy against AD.

Assessment of memory in TgCRND8 treated with D-JNK11 allowed us to test the potential of JNK inhibition on the amyloid cascade hypothesis. We used two different behavioral tests to investigate the long-term memory (novel object recognition) and the spatial learning memory (radial maze) deficits. These memory impairments correlate well with memory loss in human AD (43–45). Remarkably, D-JNK11 treatment completely reverted memory deficits in TgCRND8 mice.

Most importantly, we showed that D-JNK11 treatment reverted the hippocampal synaptic dysfunction by preventing the LTP impairment observed in TgCRND8 mice. Our data agree with those of others showing the importance of JNK signaling in LTP in aging rats as well as in models that mimic AD pathogenesis (14, 46, 47).

Our study suggests that synaptic dysfunction and memory rescue correlate with the decrease of the amyloidogenic cleavage of APP, as demonstrated by the decrease of both C-88/C-93 and  $\beta$ APP/ $\alpha$ APP ratio in TgCRND8 mice. We previously proved (18) and we confirmed here *in vivo* that D-JNK11 prevents APP668 phosphorylation and promotes the non-amyloidogenic/ $\alpha$ APP cleavage *versus* amyloidogenic/ $\beta$ APP cleavage. Others reported that APP phosphorylation in Thr-668 is regulating the conformational state of APP and consequently its intracellular homeostasis (18, 36, 48). Moreover, when phosphorylated, this residue favors the amyloidogenic/ $\beta$ APP cleavage (18, 37). It is possible that by preventing this phosphorylation *in vivo*, the APP cleavage is non-amyloidogenic/ $\alpha$ APP cleavage and the trimeric and dodecameric A $\beta$  soluble toxic forms are dramatically reduced (70–60%). As expected, such decrease in the production of toxic species correlates with recovery of synaptic functionality and memory deficits in TgCRND8 mice (3, 7, 8).

Together, the behavioral and biochemical results lead to the conclusion that JNK regulates loss of memory in a mouse model that mimics AD. Nonetheless, the role of JNK in modulating synaptic dysfunction will need further investigation.

Not surprisingly, the observed reduction on senile plaques, as a result of D-JNK11 treatment, is not as remarkable (16%) as the treatment started when small and medium plaques (4–5 months) were already present in the brain parenchyma. Overall, our results in TgCRND8 mice highlight the pivotal role of JNK in the cognitive impairment characterizing AD and set the stage for additional research on JNK as a potential therapeutic target for the treatment of AD.

*Acknowledgments*—J. Baggott kindly edited the text. We thank Cristina Ploia.

## REFERENCES

1. Sperling, R. A., Dickerson, B. C., Pihlajamaki, M., Vannini, P., LaViolette, P. S., Vitolo, O. V., Hedden, T., Becker, J. A., Rentz, D. M., Selkoe, D. J., and Johnson, K. A. (2010) *Neuromolecular Med.* **12**, 27–43
2. Soto, C. (2003) *Nat. Rev. Neurosci.* **4**, 49–60
3. Shankar, G. M., Li, S., Mehta, T. H., Garcia-Munoz, A., Shepardson, N. E., Smith, I., Brett, F. M., Farrell, M. A., Rowan, M. J., Lemere, C. A., Regan, C. M., Walsh, D. M., Sabatini, B. L., and Selkoe, D. J. (2008) *Nat. Med.* **14**, 837–842
4. Li, S., Shankar, G. M., and Selkoe, D. J. (2010) *Front Cell Neurosci.* **4**, 5
5. Lesné, S., Koh, M. T., Kotilinek, L., Kaye, R., Glabe, C. G., Yang, A., Gallagher, M., and Ashe, K. H. (2006) *Nature* **440**, 352–357
6. Cleary, J. P., Walsh, D. M., Hofmeister, J. J., Shankar, G. M., Kuskowski, M. A., Selkoe, D. J., and Ashe, K. H. (2005) *Nat. Neurosci.* **8**, 79–84
7. Lacor, P. N., Buniel, M. C., Furlow, P. W., Clemente, A. S., Velasco, P. T., Wood, M., Viola, K. L., and Klein, W. L. (2007) *J. Neurosci.* **27**, 796–807
8. Tackenberg, C., Ghori, A., and Brandt, R. (2009) *Curr. Alzheimer Res.* **6**, 261–268
9. Small, B. J., Gagnon, E., and Robinson, B. (2007) *Geriatrics* **62**, 19–23
10. Barghorn, S., Nimmrich, V., Striebing, A., Krantz, C., Keller, P., Janson, B., Bahr, M., Schmidt, M., Bitner, R. S., Harlan, J., Barlow, E., Ebert, U., and Hillen, H. (2005) *J. Neurochem.* **95**, 834–847
11. Zhu, X., Raina, A. K., Rottkamp, C. A., Aliev, G., Perry, G., Boux, H., and Smith, M. A. (2001) *J. Neurochem.* **76**, 435–441
12. Thakur, A., Wang, X., Siedlak, S. L., Perry, G., Smith, M. A., and Zhu, X. (2007) *J. Neurosci. Res.* **85**, 1668–1673
13. Morishima, Y., Gotoh, Y., Zieg, J., Barrett, T., Takano, H., Flavell, R., Davis,

- R. J., Shirasaki, Y., and Greenberg, M. E. (2001) *J. Neurosci.* **21**, 7551–7560
14. Minogue, A. M., Schmid, A. W., Fogarty, M. P., Moore, A. C., Campbell, V. A., Herron, C. E., and Lynch, M. A. (2003) *J. Biol. Chem.* **278**, 27971–27980
  15. Colombo, A., Repici, M., Pesaresi, M., Santambrogio, S., Forloni, G., and Borsello, T. (2007) *Cell Death Differ.* **14**, 1845–1848
  16. Muresan, Z., and Muresan, V. (2005) *J. Neurosci.* **25**, 3741–3751
  17. Standen, C. L., Brownlees, J., Grierson, A. J., Kesavapany, S., Lau, K. F., McLoughlin, D. M., and Miller, C. C. (2001) *J. Neurochem.* **76**, 316–320
  18. Colombo, A., Bastone, A., Ploia, C., Sclip, A., Salmona, M., Forloni, G., and Borsello, T. (2009) *Neurobiol. Dis.* **33**, 518–525
  19. Ploia, C., Antoniou, X., Sclip, A., Grande, V., Cardinetti, D., Colombo, A., Canu, N., Benussi, L., Ghidoni, R., Forloni, G., and Borsello, T. (2011) *J. Alzheimers Dis.* **26**, 315–329
  20. Vogel, J., Anand, V. S., Ludwig, B., Nawoschik, S., Dunlop, J., and Braithwaite, S. P. (2009) *Neuropharmacology* **57**, 539–550
  21. Yoshida, H., Hastie, C. J., McLaughlan, H., Cohen, P., and Goedert, M. (2004) *J. Neurochem.* **90**, 352–358
  22. Sherrin, T., Blank, T., Hippel, C., Rayner, M., Davis, R. J., and Todorovic, C. (2010) *J. Neurosci.* **30**, 13348–13361
  23. Borsello, T., Clarke, P. G., Hirt, L., Vercelli, A., Repici, M., Schorderet, D. F., Bogousslavsky, J., and Bonny, C. (2003) *Nat. Med.* **9**, 1180–1186
  24. Bonny, C., Oberson, A., Negri, S., Sauser, C., and Schorderet, D. F. (2001) *Diabetes* **50**, 77–82
  25. Chishti, M. A., Yang, D. S., Janus, C., Phinney, A. L., Horne, P., Pearson, J., Strome, R., Zuker, N., Loukides, J., French, J., Turner, S., Lozza, G., Grilli, M., Kunicki, S., Morissette, C., Paquette, J., Gervais, F., Bergeron, C., Fraser, P. E., Carlson, G. A., George-Hyslop, P. S., and Westaway, D. (2001) *J. Biol. Chem.* **276**, 21562–21570
  26. Chen, G., Chen, K. S., Knox, J., Inglis, J., Bernard, A., Martin, S. J., Justice, A., McConlogue, L., Games, D., Freedman, S. B., and Morris, R. G. (2000) *Nature* **408**, 975–979
  27. Janus, C., Pearson, J., McLaurin, J., Mathews, P. M., Jiang, Y., Schmidt, S. D., Chishti, M. A., Horne, P., Heslin, D., French, J., Mount, H. T., Nixon, R. A., Mercken, M., Bergeron, C., Fraser, P. E., St George-Hyslop, P., and Westaway, D. (2000) *Nature* **408**, 979–982
  28. Squire, L. R., Zola-Morgan, S., and Chen, K. S. (1988) *Behav Neurosci.* **102**, 210–221
  29. Olton, D. S., Meck, W. H., and Church, R. M. (1987) *Brain Res.* **404**, 180–188
  30. Hyde, L. A., Kazdoba, T. M., Grilli, M., Lozza, G., Brusa, R., Brusa, R., Zhang, Q., Wong, G. T., McCool, M. F., Zhang, L., Parker, E. M., and Higgins, G. A. (2005) *Behav. Brain Res.* **160**, 344–355
  31. Jedlicka, P., Vlachos, A., Schwarzacher, S. W., and Deller, T. (2008) *Behav. Brain Res.* **192**, 12–19
  32. Selkoe, D. J. (1991) *Sci. Am.* **265**, 68–71, 74–76, 78
  33. Francis, B. M., Kim, J., Barakat, M. E., Fraenkl, S., Yucel, Y. H., Peng, S., Michalski, B., Fahnstock, M., McLaurin, J., and Mount, H. T. (2010) *Neurobiol. Aging* [Epub ahead of print]
  34. Bellucci, A., Rosi, M. C., Grossi, C., Fiorentini, A., Luccarini, I., and Casamenti, F. (2007) *Neurobiol Dis.* **27**, 328–338
  35. Muresan, Z., and Muresan, V. (2007) *Mol. Biol. Cell* **18**, 3835–3844
  36. Ramelot, T. A., and Nicholson, L. K. (2001) *J. Mol. Biol.* **307**, 871–884
  37. Lee, M. S., Kao, S. C., Lemere, C. A., Xia, W., Tseng, H. C., Zhou, Y., Neve, R., Ahljianian, M. K., and Tsai, L. H. (2003) *J. Cell Biol.* **163**, 83–95
  38. Scheinfeld, M. H., Ghersi, E., Davies, P., and D'Adamo, L. (2003) *J. Biol. Chem.* **278**, 42058–42063
  39. Savage, M. J., Lin, Y. G., Ciallella, J. R., Flood, D. G., and Scott, R. W. (2002) *J. Neurosci.* **22**, 3376–3385
  40. Puig, B., Gómez-Isla, T., Ribé, E., Cuadrado, M., Torrejón-Escribano, B., Dalfó, E., and Ferrer, I. (2004) *Neuropathol Appl Neurobiol* **30**, 491–502
  41. Repici, M., Mare, L., Colombo, A., Ploia, C., Sclip, A., Bonny, C., Nicod, P., Salmona, M., and Borsello, T. (2009) *Neuroscience* **159**, 94–103
  42. Repici, M., Centeno, C., Tomasi, S., Forloni, G., Bonny, C., Vercelli, A., and Borsello, T. (2007) *Neuroscience* **150**, 40–49
  43. Wang, J., Dickson, D. W., Trojanowski, J. Q., and Lee, V. M. (1999) *Exp. Neurol.* **158**, 328–337
  44. McLean, C. A., Cherny, R. A., Fraser, F. W., Fuller, S. J., Smith, M. J., Beyreuther, K., Bush, A. I., and Masters, C. L. (1999) *Ann. Neurol.* **46**, 860–866
  45. Lue, L. F., Kuo, Y. M., Roher, A. E., Brachova, L., Shen, Y., Sue, L., Beach, T., Kurth, J. H., Rydel, R. E., and Rogers, J. (1999) *Am. J. Pathol.* **155**, 853–862
  46. O'Donnell, E., Vereker, E., and Lynch, M. A. (2000) *Eur. J. Neurosci.* **12**, 345–352
  47. Ramin, M., Azizi, P., Motamedi, F., Haghparast, A., and Khodagholi, F. (2011) *Behav. Brain Res.* **217**, 424–431
  48. Pastorino, L., and Lu, K. P. (2006) *Eur. J. Pharmacol.* **545**, 29–38